UNIVERSITÉ Grenoble Alpes

irstea

Sensitivity analysis of an avalanche flow dynamics model using aggregated indices

María-Belén Heredia
Ph.D. student
Supervisors: Nicolas Eckert* and Clementine Prieur+
* Irstea, Grenoble, Team ETNA
+ LJK, Univ. Grenoble Alpes, Team AIRSEA

Bordeaux, 12 November 2018.

Introduction

Avalanche event in Chamonix, France[1]

- Snow avalanches are complex phenomena.
- Avalanche models provide a simplification of the avalanche flow (equations based on mass and momentum conservation).
- The models depend on parameters poorly-known.

[1] https://www.chamonix.net/francais/events/lectures-danger-d-avalanches/5483

Introduction

Avalanche event in Chamonix, France[1]

- Snow avalanches are complex phenomena.
- Avalanche models provide a simplification of the avalanche flow (equations based on mass and momentum conservation).
- The models depend on parameters poorly-known.

Accurate estimation is needed since the knowledge of the parameter values is required for land-use planning and hazard mapping.

[1] https://www.chamonix.net/francais/events/lectures-danger-d-avalanches/5483

The avalanche model

The mass and momentum conservation equations:

$$\begin{aligned} \frac{\partial h}{\partial t} + \frac{\partial hv}{\partial x} &= 0, \\ \frac{\partial hv}{\partial t} + \frac{\partial}{\partial x}\left(hv^2 + g\frac{h^2}{2}\right) &= h\left(g\sin\theta - \mathrm{F}\right). \end{aligned}$$

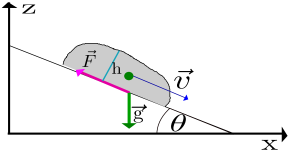

The avalanche model.

where $v = \|\vec{v}\|$ is the flow velocity, h is the flow depth, θ is the local slope, g is the gravity constant and $\mathrm{F} = \|\vec{F}\|$ is the Voellmy frictional force:

$$\mathrm{F} = \mu g cos\theta + \frac{g}{\xi h}v^2 \tag{1}$$

where μ and ξ are the friction parameters [Naaim et al., 2004].

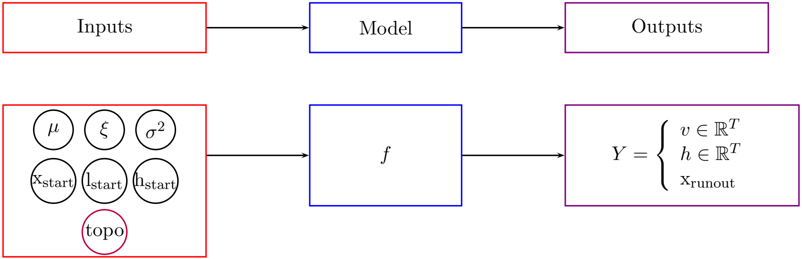

Param.	Description	Uncertainty interval
μ	Own properties of the avalanche.	0.01-0.65
ξ	Geometry of the avalanche and terrain roughness	200-10000
$\mathrm{l_{start}}$	Length of the slab at the release zone [m]	5-100
$\mathrm{h_{start}}$	Depth of the slab at the release zone [m]	0.1-4
$\mathrm{x_{start}}$ [2]	The release abscissa [m]	0.01-285
σ	Altitude Digital Elevation Model error [m]	0-0.15

Table: *Parameters description and uncertainty intervals.*

[2] Release zone average slope superior to 37°

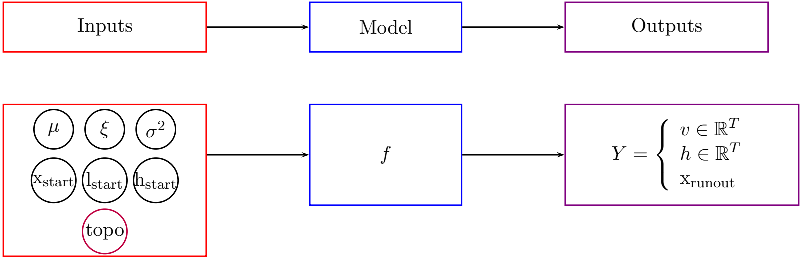

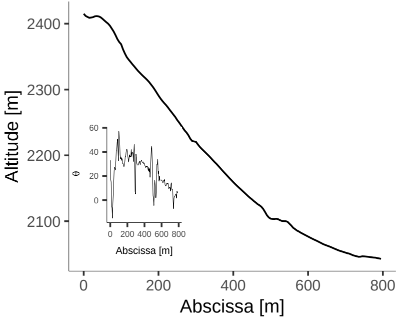

The geometry of the avalanche path 1.

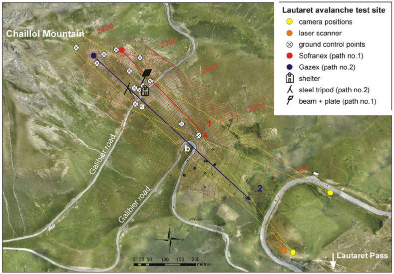

The Lautaret avalanche test site. Obtained from [Thibert et al., 2015].

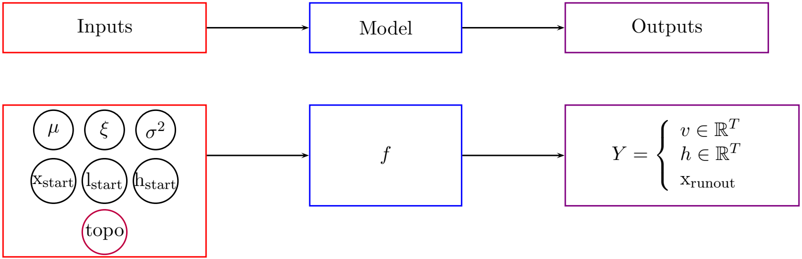

The functions v and h are discretized on the points $(x_1, \ldots, x_T) \in \mathbb{R}^T$.

v : velocity profile calculated in the discretization.
h : snow depth profile calculated in the discretization.
$\mathrm{x_{runout}}$: The runout abscissa.

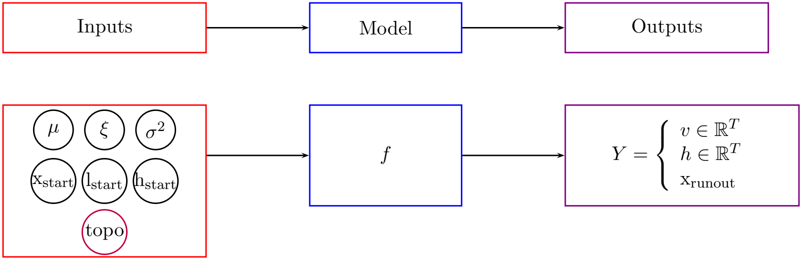

The functions v and h are discretized on the points $(x_1, \ldots, x_T) \in \mathbb{R}^T$.

v : velocity profile calculated in the discretization.
h : snow depth profile calculated in the discretization.
$\mathrm{x}_{\mathrm{runout}}$: The runout abscissa.

Outputs: 1 scalar and two vectors.

The aggregated Sobol indices

$Y = f(X)$ the p multivariate output of the model f that depends on d random inputs $X = (X_1, \dots X_d)$.

The aggregated Sobol indices

$Y = f(X)$ the p multivariate output of the model f that depends on d random inputs $X = (X_1, \ldots X_d)$.

- The random inputs $X_1, \ldots X_d$ are supposed independent.
- $\mathbb{E}(\|Y\|^2) < \infty$ where $\|\|$ is the Euclidean norm.
- The covariance matrix of Y, denoted by Σ is positive definite.

The aggregated Sobol indices

$Y = f(X)$ the p multivariate output of the model f that depends on d random inputs $X = (X_1, \ldots X_d)$.

- The random inputs $X_1, \ldots X_d$ are supposed independent.
- $\mathbb{E}(\|Y\|^2) < \infty$ where $\|\|$ is the Euclidean norm.
- The covariance matrix of Y, denoted by Σ is positive definite.

Let $u \subseteq \{1, \ldots d\}$ and $\sim u$ be its complementary in $\{1, \ldots d\}$. We set $X_u = (X_i)_{i \in u}$.
There is an unique Hoeffding decomposition of f [Hoeffding, 1948]:

$$f(X) = f_\emptyset + f_u(X_u) + f_{\sim u}(X_{\sim u}) + f_{u,\sim u}(X_u, X_{\sim u}), \quad (2)$$

where $f_\emptyset = \mathbb{E}[Y]$, $f_u = \mathbb{E}(Y|X_u) - f_\emptyset$, $f_{\sim u} = \mathbb{E}(Y|X_{\sim u}) - f_\emptyset$ and $f_{u,\sim u} = Y - f_u - f_{\sim u} - f_\emptyset$.

Thanks to the orthogonality:

$$\Sigma = C_u + C_{\sim u} + C_{u,\sim u}, \tag{3}$$

where $\Sigma, C_u, C_{\sim u}$ and $C_{u,\sim u}$ are the covariance matrices of $Y, f_u(X_u), f_{\sim u}(X_{\sim u})$ and $f_{u,\sim u}(X_u, X_{\sim u})$, respectively.

Thanks to the orthogonality:

$$\Sigma = C_u + C_{\sim u} + C_{u,\sim u}, \qquad (3)$$

where $\Sigma, C_u, C_{\sim u}$ and $C_{u,\sim u}$ are the covariance matrices of $Y, f_u(X_u), f_{\sim u}(X_{\sim u})$ and $f_{u,\sim u}(X_u, X_{\sim u})$, respectively.

Equation (3) can be projected on a scalar:

$$\mathrm{Tr}(\Sigma) = \mathrm{Tr}(C_u) + \mathrm{Tr}(C_{\sim u}) + \mathrm{Tr}(C_{u,\sim u}), \qquad (4)$$

where Tr denotes the trace operator.

Thanks to the orthogonality:

$$\Sigma = C_u + C_{\sim u} + C_{u,\sim u}, \tag{3}$$

where $\Sigma, C_u, C_{\sim u}$ and $C_{u,\sim u}$ are the covariance matrices of $Y, f_u(X_u), f_{\sim u}(X_{\sim u})$ and $f_{u,\sim u}(X_u, X_{\sim u})$, respectively.

Equation (3) can be projected on a scalar:

$$\mathrm{Tr}(\Sigma) = \mathrm{Tr}(C_u) + \mathrm{Tr}(C_{\sim u}) + \mathrm{Tr}(C_{u,\sim u}), \tag{4}$$

where Tr denotes the trace operator.

If $\mathrm{Tr}(\Sigma) \neq 0$, the aggregated Sobol indice with respect to u is defined as [Gamboa et al., 2013, Lamboni et al., 2011]:

$$0 \leq S^u(f) = \frac{\mathrm{Tr}(C_u)}{\mathrm{Tr}(\Sigma)} \leq 1 \tag{5}$$

Functional Principal Component Analysis

Aim: To approximate the sample function e.g., $v_1, \dots, v_N \in \mathbb{R}^T$ on an basis $\Psi_{T\times K}$ where $K \leq T$:

$$v_j(x) \approx \overline{v}(x) + \sum_{k=1}^{K} \alpha_{j,k}^{(v)} \psi_k^{(v)}(x) \tag{6}$$

where $x \in \mathbb{R}^+$, $j \in \{1, \dots N\}$, $\overline{v}(x)$ is the mean of $\{v_1(x), \dots, v_N(x)\}$, and $\alpha_{j,k}^{(v)}$ is the coefficient of the jth on the kth component.

Functional Principal Component Analysis

Aim: To approximate the sample function e.g., $v_1, \ldots, v_N \in \mathbb{R}^T$ on an basis $\Psi_{T\times K}$ where $K \leq T$:

$$v_j(x) \approx \overline{v}(x) + \sum_{k=1}^{K} \alpha_{j,k}^{(v)} \psi_k^{(v)}(x) \tag{6}$$

where $x \in \mathbb{R}^+$, $j \in \{1, \ldots N\}$, $\overline{v}(x)$ is the mean of $\{v_1(x), \ldots, v_N(x)\}$, and $\alpha_{j,k}^{(v)}$ is the coefficient of the jth on the kth component.

The method proposed by [Ramsay and Silverman, 2005] searches for the basis functions $\psi_1^{(v)}, \ldots \psi_K^{(v)}$ and the coefficients $\alpha_{j,k}^{(v)}$, $j \in \{1, \ldots n\}, k \in \{1, \ldots K\}$ that minimizes:

$$\sum_{j=1}^{N} \int_{\mathbb{R}+} \left(v_j(x) - \overline{v}(x) - \sum_{k=1}^{K} \alpha_{j,k}^{(v)} \psi_k^{(v)}(x) \right)^2 dx, \tag{7}$$

such that the functions $\psi_1^{(v)}, \ldots, \psi_K^{(v)}$ are orthonormal.

Solution: To apply PCA to $\hat{Y}$, the sample functions evaluated in the discretized points $x_1, \dots x_T \in \mathbb{R}^+$
([Lamboni et al., 2011, Nanty et al., 2017, Ramsay and Silverman, 2005]).

$$\hat{Y} = \begin{bmatrix} v_1(x_1)/N_v & \dots & v_1(x_T)/N_v & h_1(x_1)/N_h & \dots & h_1(x_T)/N_h & x_{\text{runout},1}(x_1)/N_{x_{\text{runout}}} \\ \vdots & & \vdots & & \vdots & & \vdots \\ v_N(x_1)/N_v & \dots & v_N(x_T)/N_v & h_N(x_1)/N_h & \dots & h_N(x_T)/N_h & x_{\text{runout},1}(x_N)/N_{x_{\text{runout}}} \end{bmatrix}$$

where:

$$N_v = \max_{\substack{1 \le j \le N \\ 1 \le t \le T}} v_j(x_t), \tag{8}$$

and similar for N_h and $N_{x_{\text{runout}}}$.

The PCA decomposition of $\hat{Y}$ is based on the expansion of Σ', the variance-covariance matrix of $\hat{Y}$:

$$\Sigma' = \sum_{k=1}^{2\times T+1} u_k \mathbf{v}_k \mathbf{v}_k^T \tag{9}$$

with $u_1 \geq \ldots \geq u_q$ the eigenvalues of Σ' and $\mathbf{v}_1, \ldots, \mathbf{v}_p$ a set of normalized and mutually orthogonal eigenvectors associated to these eigenvalues. We have the approximation:

$$\hat{Y} \approx \mathbb{E}\hat{Y} + \sum_{k=1}^{K} h_k \mathbf{v}_k \tag{10}$$

where $K \leq 2 \times T + 1$.

The aggregated Sobol indices are calculated on $H = [h_1, ..., h_K]$.

Technical details

The R package [R Core Team, 2017] **sensitivity** developed by [Pujol et al., 2017] is used to calculate the indices and we used the estimation proposed by [Tissot and Prieur, 2015]. 20.000 model simulations were made to estimate the indices.

The Scalar Sobol indices

a) x_{runout} *distance*

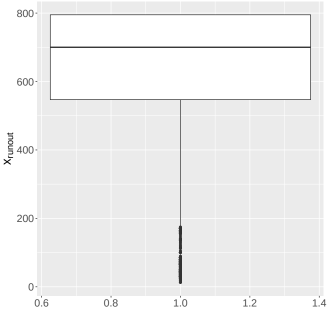

b) x_{dist} *Scalar Sobol indice*

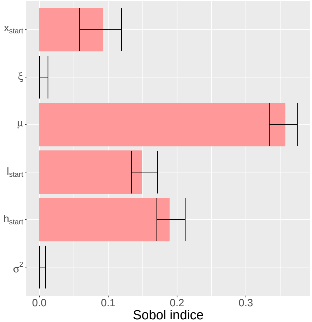

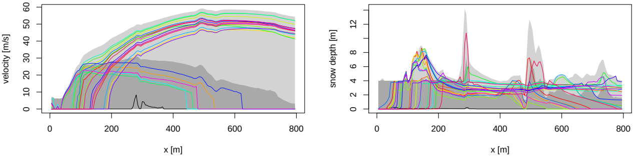

FHDR **boxplots** of the velocity and the snow depth outputs.

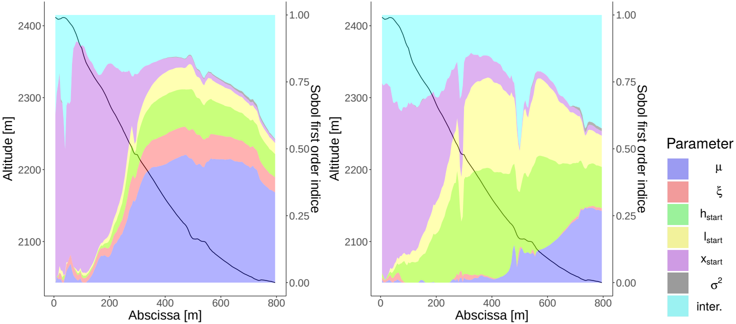

Scalar Sobol indices of the vector whose components are the evaluation of the functional velocity and snow depth. The avalanche path is shown with a black line.

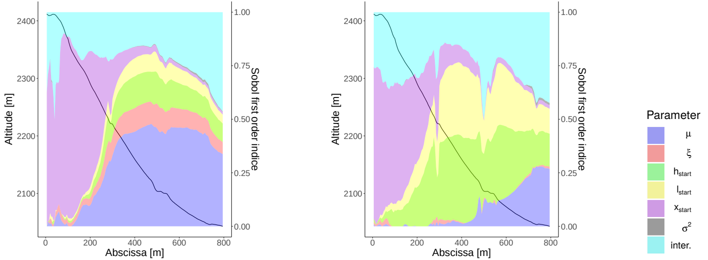

Scalar Sobol indices of the vector whose components are the evaluation of the functional velocity and snow depth. The avalanche path is shown with a black line.

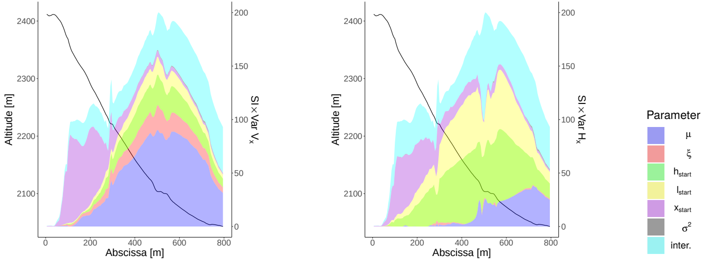

The product between the scalar Sobol indice and the variance of the vector whose components are the evaluation of the functional velocity and snow depth on a grid.

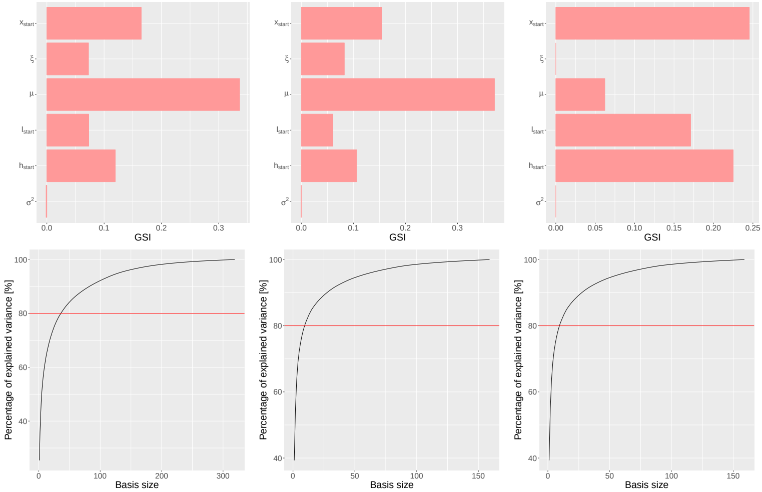

All the output *The velocity output* *The snow depth output*

Upper panel: The aggregated Sobol indice. **Lower panel:** The percentage of explained variance in function of the number of PCs.

Conclusions

- The scalar Sobol indices provide useful information about the parameters sensitivity but redundant.
- The aggregated Sobol indices summarize the importance of the model parameters.
- The parameter μ is the most influential parameter to the velocity output.
- The parameters x_{start}, l_{start} and h_{start} are the most influential to the snow depth output.

Perspectives

- To perform a similar sensitivity analysis in other paths to generalize the results.
- To use a more complex dynamic avalanche model (e.g., potentially 3-D).

Thank you.

The Highest Density Region plot

Tool for visualizing large amounts of functional data based in the estimation of the bivariate kernel density function of the two first components of the decomposition of the functional data Y [Hyndman and Shang, 2010]:

$$\hat{f}(z) = \frac{1}{n} \sum_{i=1}^{n} K_{h_i}(z - Z_i), \tag{11}$$

where $z \in \mathbb{R}^2$, $Z = \{Z_1, \ldots, Z_n\} \in \mathbb{R}^2$ is the set of bivariate scores of the PCA, K is a kernel function and h_i is a bandwidth for the ith dimension.
The HDR (Highest Density Region) is defined as:

$$R_\alpha = \{z \in \mathbb{R}^2 : \hat{f}(z) \geq f_\alpha\} \tag{12}$$

where f_α is such that $\int_{R_\alpha} \hat{f}(z)dz = 1 - \alpha$.

The HDR boxplot shows:

- The regions of highest density $\alpha = 0.5$ (light gray) and $\alpha = 0.99$ (dark gray).
- The outliers defined as the points that do not belong to these two regions (color lines).
- The mode (the curve with the highest density, black line).

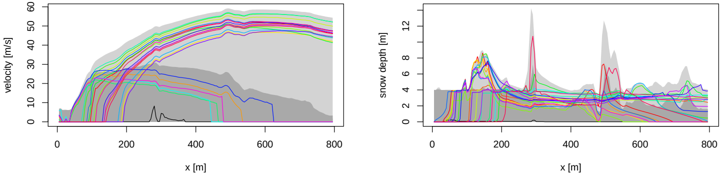

Functional HDR boxplots for the velocity (left panel) and snow depth (right panel)

Back to the presentation.

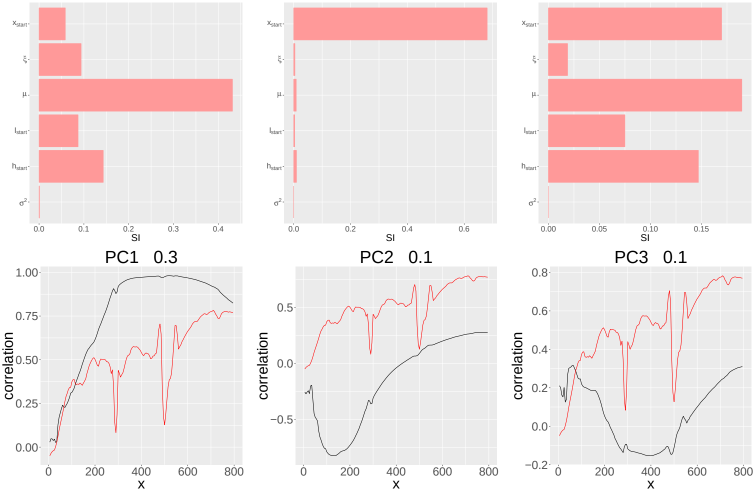

Using all the output output. Upper pannel: The first three principal components, the black line corresponds to the correlation between the PC and the output. Lower pannel: The first order Sobol indices of the first three principal components.

References I

Gamboa, F., Janon, A., Klein, T., and Lagnoux, A. (2013).
Sensitivity analysis for multidimensional and functional outputs.
ArXiv e-prints.

Hoeffding, W. (1948).
A class of statistics with asymptotically normal distribution.
The Annals of Mathematical Statistics, 19(3):293–325.

Hyndman, R. J. and Shang, H. L. (2010).
Rainbow plots, bagplots, and boxplots for functional data.
Journal of Computational and Graphical Statistics, 19(1):29–45.

Lamboni, M., Monod, H., and Makowski, D. (2011).
Multivariate sensitivity analysis to measure global contribution of input factors in dynamic models.
Reliability Engineering & System Safety, 96(4):450 – 459.

Naaim, M., Naaim-Bouvet, F., Faug, T., and Bouchet, A. (2004).
Dense snow avalanche modeling: flow, erosion, deposition and obstacle effects.
Cold Regions Science and Technology, 39(2):193 – 204.
Snow And Avalanches: Papers Presented At The European Geophysical Union Conference, Nice, April 2003. Dedicated To The Avalanche Dynamics Pioneer Dr. B. Salm.

References II

Nanty, S., Helbert, C., Marrel, A., Pérot, N., and Prieur, C. (2017).
Uncertainty quantification for functional dependent random variables.
Computational Statistics, 32(2):559–583.

Pujol, G., Iooss, B., with contributions from Khalid Boumhaout, A. J., Veiga, S. D., Delage, T., Fruth, J., Gilquin, L., Guillaume, J., Le Gratiet, L., Lemaitre, P., Nelson, B. L., Monari, F., Oomen, R., Ramos, B., Roustant, O., Song, E., Staum, J., Touati, T., and Weber, F. (2017).
sensitivity: Global Sensitivity Analysis of Model Outputs.
R package version 1.15.0.

R Core Team (2017).
R: A Language and Environment for Statistical Computing.
R Foundation for Statistical Computing, Vienna, Austria.

Ramsay, J. O. and Silverman, B. W. (2005).
Functional Data Analysis.
Springer Series in Statistics. Springer, 2nd edition.

Thibert, E., Bellot, H., Ravanat, X., Ousset, F., Pulfer, G., Naaim, M., Hagenmuller, P., Naaim-Bouvet, F., Faug, T., Nishimura, K., Ito, Y., Baroudi, D., Prokop, A., Schon, P., Soruco, A., Vincent, C., Limam, A., and Héno, R. (2015).
The full-scale avalanche test-site at Lautaret Pass (French Alps).
Cold Regions Science and Technology, 115:30 – 41.

References III

Tissot, J.-Y. and Prieur, C. (2015).
A randomized Orthogonal Array-based procedure for the estimation of first- and second-order Sobol' indices.
Journal of Statistical Computation and Simulation, 85(7):1358–1381.